Chapter 3

Experimental design (Materials and Methods)

This chapter outlines the synthesis route and characterizations of piezoelectric sodium potassium niobates [$Na_xK_{1-x}NbO_3$ (x = 0.2-0.8), NKN] and hydroxyapatite ceramics. Phase evolution and microstructural characterization techniques are described. Surface chemistry evaluation and physical characterization techniques such as X-ray photoelectron spectroscopy and contact angle measurement are also discussed. Cell culture studies are performed to investigate the influence of surface modification (polarization) and external electrical stimulation on the biocompatibility of NKN ceramics. The techniques, involved in the evaluation of the antibacterial response of surface polarized NKN are also discussed. In vivo study is also performed to examine the toxicity of NKN nanoparticles in the rat model.

3.1. Synthesis

3.1.1. Synthesis of sodium potassium niobates [$Na_xK_{1-x}NbO_3$ (x = 0.2 - 0.8), NKN]

$Na_xK_{(1-x)}NbO_3$ was prepared via solid state synthesis method, in which Na_2CO_3 (Sigma Aldrich, 99%), K_2CO_3 (Sigma Aldrich, 99%) and Nb_2O_5 (Sigma Aldrich, 99.5%) were used as precursors [1]. The stoichiometric amounts of precursors were ball milled in ethanol medium for 24 h with zirconia balls (ball to powder weight ratio; 4:1) in high density polyethylene (HDPE) jar (Fig. 3.1). The obtained wet slurry was dried in an oven overnight followed by crushing using agate mortar pestle. The dried powder was calcined at 910 °C for 10 h. The calcined powder was again ball milled for 16 h to further reduce the particle size after calcination.

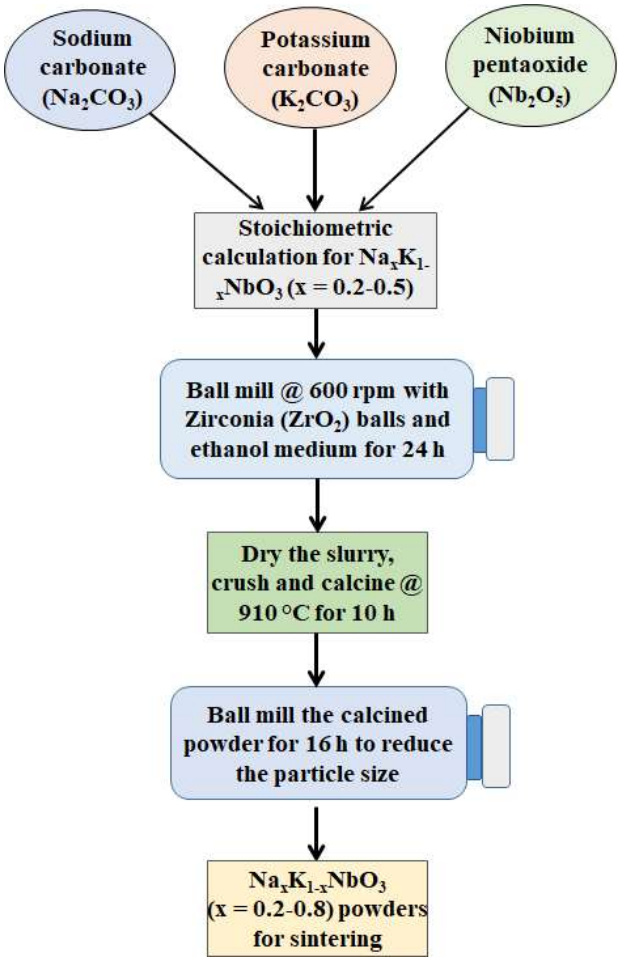

Fig. 3.1. Flow chart for the synthesis of $Na_xK_{(1-x)}NbO_3$ (x = 0.2, 0.5 and 0.8).

During calcination, the formation of $Na_xK_{(1-x)}NbO_3$ (x = 0.2, 0.5 and 0.8) occurs as follows (Eqns. 3.1, 3.2 and 3.3),

$$\frac{1}{10}Na_2CO_3 + \frac{4}{10}K_2CO_3 + \frac{1}{2}Nb_2O_5 \rightarrow Na_{0.2}K_{0.8}NbO_3 + \frac{1}{2}CO_2 \quad (3.1)$$

$$\frac{1}{4}Na_2CO_3 + \frac{1}{4}K_2CO_3 + \frac{1}{2}Nb_2O_5 \rightarrow Na_{0.5}K_{0.5}NbO_3 + \frac{1}{2}CO_2 \quad (3.2)$$

$$\frac{2}{5}Na_2CO_3 + \frac{1}{10}K_2CO_3 + \frac{1}{2}Nb_2O_5 \rightarrow Na_{0.8}K_{0.2}NbO_3 + \frac{1}{2}CO_2 \quad (3.3)$$

3.1.2. Synthesis of hydroxyapatite (HA)

The biocompatible hydroxyapatite (HA) was used as a control sample. HA was synthesized via coprecipitation method using calcium oxide (CaO, Merck, 99 %) and orthophosphoric

acid (H_3PO_4, Himedia) as precursors [2]. In this route, the aqueous solution of H_3PO_4 was mixed dropwise in CaO solution with a magnetic stirrer. The temperature and pH of the solution were kept at 80 °C and 8 - 10, respectively. The precipitated solution was kept for a day, filtered and dried at 100 °C. The dried substance was crushed properly and the powder was calcined at 800 °C for 2 h.

3.2. Consolidation of synthesized $Na_xK_{(1-x)}NbO_3$ and HA powders

The synthesized NNK and HA powders were then compacted into disc shape (diameter: 10 mm, thickness: 1 mm) via uniaxial pressing 5 MPa, followed by cold isostatic pressing (CIP) at the pressure of ~330 MPa [Fig. 3.2]. CIP has been recognized to produce dense piezoelectric NKN ceramics [3]. The disc samples of $Na_xK_{(1-x)}NbO_3$ and HA were sintered in the optimized temperature range. Table 3.1 shows the optimized sintering parameters for $Na_xK_{(1-x)}NbO_3$ (x = 0.2 - 0.8) and HA samples.

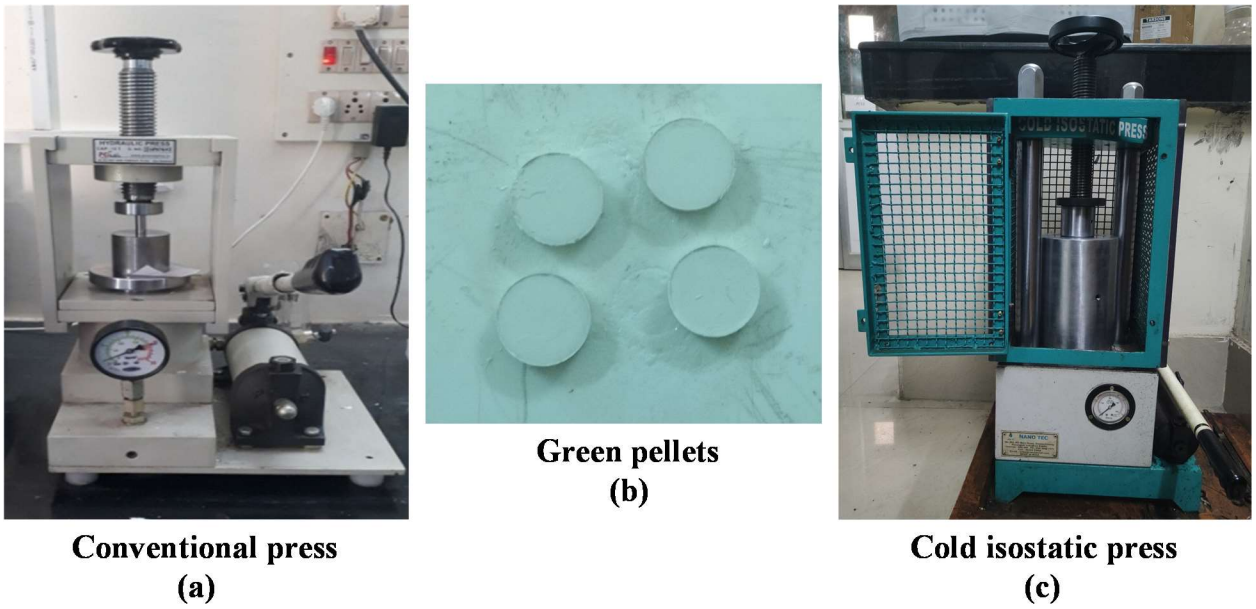

Fig. 3.2. Digital images of (a) Conventional press, (b) Green pellets, (c) Cold isostatic press.

Table 3.1. Sintering parameters, optimized for the developed compositions

S. No.	Samples	Sintering temperature (ºC)	Duration (h)	Heating rate (°C/min)
1.	$Na_xK_{1-x}NbO_3$ (x = 0.2) or $Na_{0.2}K_{0.8}NbO_3$	1010	2	5
2.	$Na_xK_{1-x}NbO_3$ (x = 0.5) or $Na_{0.5}K_{0.5}NbO_3$	1075	2	5
3.	$Na_xK_{1-x}NbO_3$ (x = 0.8) or $Na_{0.8}K_{0.2}NbO_3$	1120	2	5
4.	Hydroxyapatite (HA)	1200	2	5

3.3. Characterization

3.3.1. X-ray diffraction (XRD) analyses

The phases of sintered NKN and HA samples were analyzed by X-ray diffraction (XRD, Rigaku Miniflex II Desktop X-ray Diffractometer) technique with Cu-Kα (wavelength, λ = 1.5406 Å). The data was collected over the diffraction angle range of 20 – 60 ° (scan rate: 2 °/min) in the step size of 0.02 °. Rietveld analyses (using Full Prof Suit program) was performed from XRD data, to retrieve the information on structural changes with compositional variation in $Na_xK_{1-x}NbO_3$. XRD patterns were also analyzed via X-ray peak profile analyses via the broadening of intense peaks. Crystallite size and strain were evaluated using various methods such as Scherrer, modified Scherrer, Williamson-Hall plot, size-strain and Halder-Wagner methods.

The crystallite size was calculated using Scherrer formula (Eqn. 3.4) for $Na_xK_{1-x}NbO_3$ ceramic samples as.

$$D = \frac{k\lambda}{\beta Cos\theta} \qquad (3.4)$$

Where, *D, β, λ, k* and θ are crystallite size (in nm), FWHM (in radians), wavelength of X-ray (1.5406 Å), shape factor (0.94) and Bragg's diffraction angle (in radians), respectively.

The modified Scherrer method consider each peak during the measurement of crystallite size and therefore, reduced the error in measurements. By taking $\log_e$ on both side of Eqn. (3.4), we get,

$$\ln \beta = \ln\left(\frac{k\lambda}{D}\right) + \ln\left(\frac{1}{\cos\theta}\right) \qquad (3.5)$$

Williamson Hall plot method demonstrates the size and strain induced deformation with considerable peak broadening. Therefore, total peak broadening will be the sum of size and strain induced broadening of peaks [4].

Therefore,
$$\beta = \beta_D + \beta_\varepsilon \qquad (3.6)$$

$$\beta \cos\theta = \left(\frac{k\lambda}{D}\right) + 4\varepsilon \sin\theta \qquad (3.7)$$

Where, D and ε represent the values of crystallite size and lattice strain, respectively.

In size-strain plot method, Lorentz and Gaussian functions illustrate the profiles of crystallite size and strain, respectively [5, 6, 7]. Therefore, the total broadening of size-strain plot is the sum of Lorentz and Gaussian functions i.e., $\beta = \beta_L + \beta_G$, where, β_L and β_G are the broadening of peaks for Lorentz and Gaussian functions, respectively.

According to size-strain plot method,

$$(d\beta \cos\theta)^2 = \left(\frac{k\lambda}{D}\right)(d^2\beta \cos\theta) + \left(\frac{\varepsilon}{2}\right)^2 \qquad (3.8)$$

Where, d is interplanar spacing.

3.3.2. Fourier transform infrared (FTIR) spectroscopy

The functional groups, present in the sintered samples were identified by tracing Fourier transform infrared spectra with FTIR Spectrometer (Bruker Tensor 27, Germany) over the wavenumber range of 4000 to 400 cm^{-1} in transmission mode.

3.3.3. Microstructural analyses

The particle size and morphology of calcined $Na_xK_{(1-x)}NbO_3$ powders were analyzed through scanning electron microscopy (SEM, Evo 18, Zeiss). The energy-dispersive X-ray spectroscopy (EDS) was used for elemental analyses. The microstructure of fractured disc samples was also examined using SEM. For this purpose, the mirror-polished samples were thermally etched. Thereafter, the pellets were broken after dipping in liquid nitrogen and the fractured surface of the pellets were examined using SEM. The powders and pellets were gold sputtered prior to SEM analyses.

3.4. Densification and mechanical property measurement

Archimedes' principle was used to measure the densification of sintered $Na_xK_{1-x}NbO_3$ and HA samples. The resistance of fabricated samples against indentation, abrasion or penetration is termed as hardness. The hardness of prepared ceramic pellets was measured using Vicker's hardness tester (Digi-test, VTP-6046) with applied load and dwell time of loading of 50 N and 10 s, respectively. The dimension of the circular pellets was kept as diameter: 10 mm, thickness: 2 mm and a diamond indenter of pyramidal shape was used for operation. The experiment was performed using the standard protocol, illustrated as ASTM E384 [8] using the formula (Eqn. 3.9),

$$H_v = 1.854\frac{F}{d^2} \qquad (3.9)$$

Where, F and d indicate the applied load (N) and average diagonal length, respectively. The mean value of three to five indentations for each pellet was used for comparison.

The compressive strength of $Na_xK_{1-x}NbO_3$ and HA samples was measured using a universal testing machine (Tinius Olsen). The test was performed according to ASTM C773, specialized for compression test. The size of circular pellets was kept as hight:15 mm, diameter:10 mm and the feed speed of cross head was set as 0.5 mm/min. The ultimate compressive strength was calculated using the following formula (Eqn. 3.10),

$$\sigma_C = \frac{Applied\ load\ (N)}{cross\ sectional\ area\ (mm^2)} \qquad (3.10)$$

3.5. Ion leaching study of NKN samples in simulated body fluid (SBF)

To understand the actual leaching behavior of prepared compositions of $Na_xK_{1-x}NbO_3$ in biological fluid, the ion leaching study was performed. For this purpose, the concentration of leached ions such as Na^+, K^+ from NKN pellets in SBF (pH; 7.4, prepared by Kokubo's method) [9] was measured using ICP-AES (iCAP 6000 Series, Thermofisher Scientific). The sintered pellets of $Na_xK_{1-x}NbO_3$ were kept in SBF (10 mg/ml) for 7, 14 and 21 days at 37 °C. The solution's pH was maintained at 7.4 throughout the experiment. After the specified period of time, the obtained solutions from each sample were diluted 10 times in ultrapure water and then filtered using 0.2-micron sterile filter, before measurements.

3.6. Polarization treatment of the samples

The sintered samples of $Na_xK_{1-x}NbO_3$, as well as HA, were properly finished with emery paper, followed by diamond polishing. The polarization of polished samples was performed by corona poling at temperature and voltage of 500 °C and 25 kV, respectively, for 30 min [Fig. 3.3 (a)]. The distance between the surface of sample and corona tip was kept to about 1 cm. Further, the samples were cooled down under the constant exposure of applied voltage.

The surface of the pellet with the direct exposure of corona was negatively polarized (Neg. Pol.) and the opposite surface was positively polarized (Pos. Pol.).

3.7. Surface charge measurement

In order to evaluate the charge, stored in the polarized $Na_xK_{1-x}NbO_3$ pellets and to investigate the influence of polarization on the crystal structure, TSDC measurement was performed. For this purpose, the polarized NKN samples were depolarized by heating the pellets from room temperature to 500 °C, with a heating rate of 5 °C/min up. During this period, TSDC spectrum was recorded using a Femto/Picoammeter (B2981A, Keysight) [Fig. 3.3 (b)].

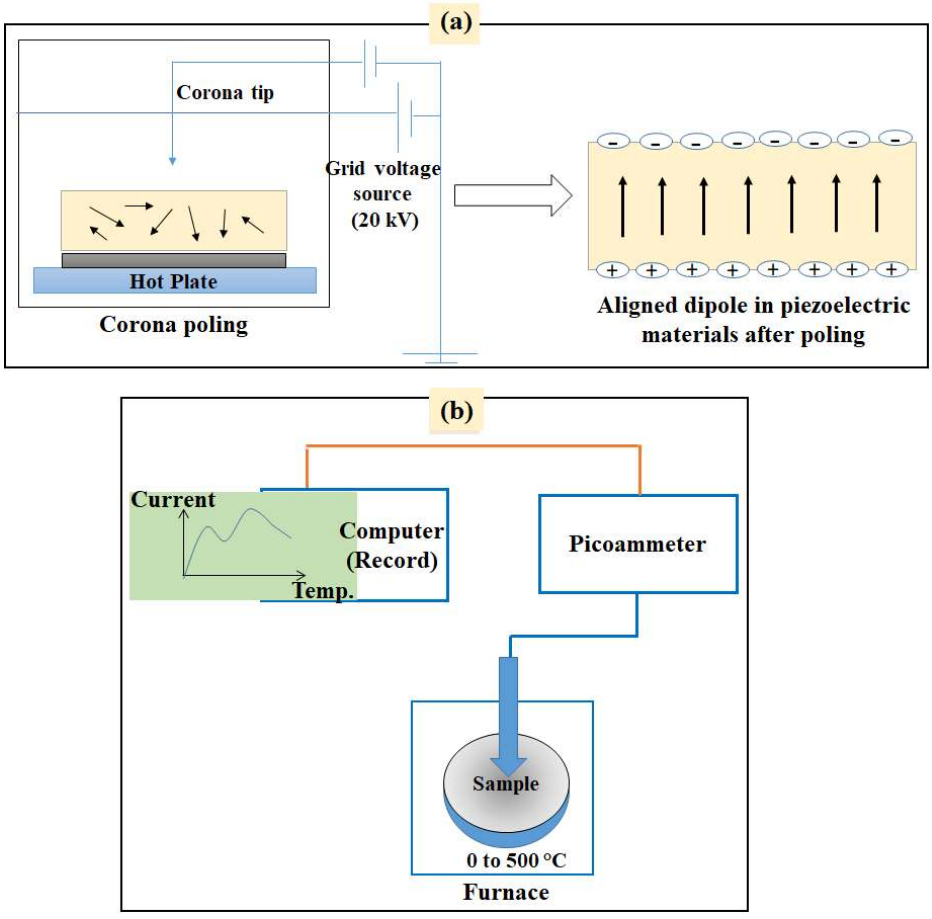

Fig. 3.3. Surface charge polarization and measurement of thermally stimulated depolarized current. (a) Schematic illustration of high voltage (25 kV) corona poling unit for the development of electrical charges on the surface of the specimen. (b) Schematic shows the

thermally stimulated depolarized current measurement setup includes picoammeter, furnace and simulator.

3.8. X-ray photoelectron spectroscopy (XPS)

XPS analyses was performed to understand the influence of polarization on the surface chemistry of the $Na_{0.5}K_{0.5}NbO_3$ sample. The survey spectra for non-polarized (non Pol.) and polarized samples were scanned using an X-ray photoelectron spectrometer (Thermo Fisher Scientific).

3.9. Physical characterization (Contact angle measurement)

The contact angle on the non-polarized and polarized $Na_xK_{1-x}NbO_3$ and HA samples were examined with deionized water and cell media to observe the influence of surface charge polarization on the hydrophilicity. For this purpose, a contact angle measurement setup (KRUSS GmbH Germany, model DSA10) was used. The hydrophilic surfaces are more favorable for the attachment and spreading of cells as compared to hydrophobic surfaces [10].

3.10. Cellular response

Cell culture experiments have been performed to evaluate the viability of MG-63 and human mesenchymal stem cells (hMSCs) on the non-Pol. and polarized $Na_xK_{1-x}NbO_3$ and HA (control). MG-63, the human osteosarcoma cells, were procured from (NCCS Pune, Maharashtra) and hMSCs (HiFi^{TM}) were obtained from Himedia labs. The MG-63 cells were cultured at 37 $^{\circ}$C (5 % CO_2 and relative humidity: 95 %) in DMEM medium (Dulbecco's modified eagle medium, high glucose powder) supplemented with fetal bovine serum (15 %) and antibiotics (1 %, Antibiotic-Antimycotic). However, hMSCs were grown in expansion media (HiMesoXL™) with a similar supplementary medium and environment. In the

confluent layer of cells, a small amount of 0.25 % Trypsin - EDTA solution was added to the culture flask for the detachment of cells from the surface. The viable cells were counted using hemocytometer and Axiovert 25 microscope (Carl Zeiss AG). After counting, 2×10^4 cells/ml were seeded on each sample and then incubated in the respective medium at 37 $^{\circ}$C (5 % CO_2 and relative humidity: 95 %). The culture medium was replaced with fresh media after every 48 to 72 h. To observe the effect of external electrical stimulation, pulsed electric field (1 V/cm for a pulse duration of 400 µs) was applied on the cells after 12 and 24 h of seeding with a digital oscilloscope (SMO702, ScientiFic) [Fig. 3.4].

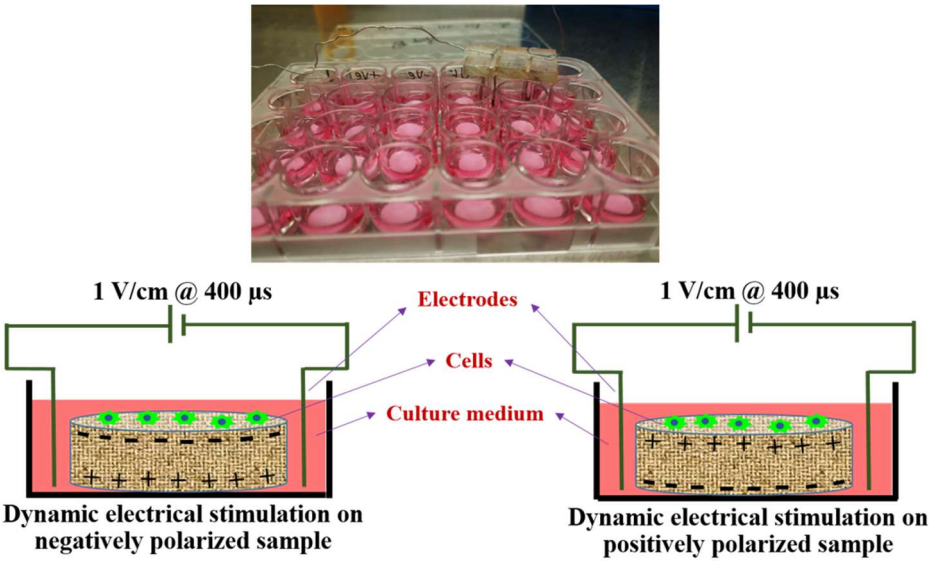

Fig. 3.4. Schematic demonstrating the synergistic action of surface charge polarization and external electrical stimulation during cell culture experiment. The application of dynamic electrical stimulation (1 V/cm, 400 µs), while cells are being adhered on the (c) Neg. Pol. (d) Pos. Pol. surfaces.

3.10.1. Quantitative analyses

3.10.1.1. MTT assay

Generally, MTT [3-(4, 5-dimethylthiazol-2-yl)-2, 5-diphenyl-tetrazolium- bromide)] assay is used to observe cell growth on the biomaterials. Cell proliferation study was performed using

MG-63 and hMSCs cells, after 3, 5 and 7 days of culture on the non-Pol. and polarized $Na_xK_{1-x}NbO_3$ samples as well as HA control. After the stipulated incubation period, the growth media was removed from each sample. After rinsing with PBS (phosphate buffer saline), the reconstituted MTT (MTT: media ratio kept at 1:10) was added to each sample and again incubated for 6 h, at 37 $^{\circ}$C (5 % CO_2 and relative humidity: 95 %) to permit the formation of formazan crystals by reacting live cells with reconstituted MTT. Thereafter, the obtained solution was replaced with dimethyl sulfoxide (DMSO) for the dissolution of formazan crystals. Further, the concentration of these formazan crystals was measured as optical density using ELISA microplate (iMark Bio-red) reader, at 595 nm. The outcomes, obtained from the samples were statistically analyzed using SPSS (IBM) software. The significant differences among the examined samples were analyzed using ANOVA technique. Tukey and Games-Howell tests, at $p < 0.05$, were used for the Post Hoc multiple comparisons.

3.10.1.2. Alkaline phosphatase (ALP) activity

ALP assay was used for the assessment of the osteogenic potential of the developed scaffolds with MG-63 cells, after 7 and 14 days of incubation. ALP activity is an early biomarker of osteoblast differentiation and therefore, indicates the neo bone forming ability on the seeded scaffolds [11, 12]. Moreover, ALP activity depicts several precise biological processes including the initiation of biomineralization etc. [12, 13]. The osteogenic culture media was prepared by adding 0.2 mM L-ascorbic acid and 10 mM β-Glycerol phosphate in DMEM supplemented with FBS and antibiotics. The non-Pol. and polarized $Na_xK_{1-x}NbO_3$ and control samples were seeded with MG-63 cells, at a density of 2×10^4 cells/ml. The seeded samples were incubated in the prepared osteogenic culture media in a CO_2 incubator (5 %

CO_2 and relative humidity: 95 %). The electrical stimulation (1 V/cm with a pulse duration of 400 μs) was applied on the wells after 12 and 24 h of incubation to observe the effect of dynamic electrical stimulation on the ALP activity. After stipulated period of time, the seeded cells were lysated using Triton X-100 (50μl of 0.1 %) for 5 min. Subsequently, 200 μl of *p*-nitrophenyl phosphate (PNP) was added to each sample and further incubated for 1 h at 37 °C. After that, the reaction was ceased by the addition of 2 N NaOH (100 μl). Finally, the absorbance of the obtained solution was taken in triplicate at 405 nm using ELISA microplate reader. The ALP activities of the samples were normalized with BSA standard curve.

3.10.2. Morphological analyses of adhered cells

The adhesion and morphology of hMSCs cells on $Na_xK_{1-x}NbO_3$ samples and control were observed using fluorescence microscopy. After 3 days of seeding, the cells, adhered on the samples were fixed using paraformaldehyde and then permeabilized with Triton X-100. These permeabilized cells were blocked by the addition of bovine serum albumin (BSA). Thereafter, the nuclei and cytoskeletons were stained with DAPI and Alexafluor dyes, respectively. The stained cells were observed using fluorescence microscope. The projected areas of 20 randomly selected adhered cells were measured using Image J software.

3.10.3. Intracellular Ca^{2+} ions measurement

It has been suggested that electrical stimulation activates the voltage gated calcium channels and thereby, allowing a larger influx of extracellular Ca^{2+} to the cells which consequently, increases intracellular Ca^{2+} [14, 15]. Such a rise in the concentration of intracellular Ca^{2+} promotes the transforming growth factor and bone morphogenetic protein through the activation of gene transcription [14, 15]. Therefore, the external electrical stimulation

induced augmentation in intracellular Ca^{2+}, helps in regulating cellular metabolism. It has also been suggested that, the intracellular Ca^{2+} are second messenger and are responsible for optimal cellular functionality and bone remodeling [16, 17, 18, 19]. In the present study, the intracellular calcium ions measurement has been performed to understand the influence of surface polarization and external electrical stimulation after seeding the MG-63 cells on the $Na_xK_{1-x}NbO_3$ and control samples. Fura-2 acetoxymethylester (Fura-2 AM, Thermofisher scientific), an intracellular Ca^{2+} indicator dye was used which is based on the ratiometric method of measurement. In this experiment, the cells were seeded on the non-Pol. and polarized $Na_xK_{1-x}NbO_3$ and HA samples in 24 well plates, followed by the application of dynamic electrical stimulation (after 12 and 24 h). After 48 h of seeding, the culture media was removed and the samples were washed using HEPES buffered saline (HBS) solution, containing 1 mM $MgCl_2$, 5 mM KCl, 1 mM $CaCl_2$, 145 mM NaCl, 10 mM HEPES, 10 mM glucose (pH; 7.4). Thereafter, dye solution (containing HBS, 0.1% BSA, 5 μM fura-2 AM) was added to each sample and the samples were then incubated in dark. After 1 h, the dye solution was removed from each sample and washed with HBS. Following this, HBS solution, supplemented with probenecid (2.5 mM) was added to each sample and incubated of 20 min. in dark. Probenecid prevents the leakage of Fura-2 AM dye from the cells [20].The solution from each well was transferred to the black colored 96 well plate and the reading was taken at the emission intensity of 510 nm. The excitation intensity was set at 340 and 380 nm as Fura-2 AM dye gives maximum fluorescence emission intensity with and without intracellular Ca^{2+} at the excitation wavelengths of 340 and 380 nm, respectively. Therefore, the ratio of the measured fluorescence intensity of Fura-2 AM at the excitation wavelengths of 340 (calcium bound) and 380 nm (calcium free) is directly proportional to the

amount of intracellular calcium ions. The reading was taken at the interval of 10 s for 10 cycles using florescence plate reader (Synergy H1).

3.11. Antibacterial response

The antibacterial performance of $Na_xK_{1-x}NbO_3$ (x = 0.2 to 0.8) samples was examined against gram-negative (*E. coli.)* and gram-positive *(S. aureus)* bacteria by considering HA as control. Quantitative assessment was made by MTT [3-(4, 5-dimethylthiazol-2-yl)-2, 5-diphenyl tetrazolium bromide] assay, while qualitative analysis was performed using fluorescence microscopy and disk diffusion methods. In addition, enzymatic activities were also observed to estimate the amount of ROS, produced on the samples, while cultured with bacteria. Gram-negative (*E. coli)* and gram-positive *(S. aureus)* bacteria were procured from Microbial Type Culture Collection (MTCC) Chandigarh, India. The bacteria were grown in nutrient broth for 12 h at 37 °C to obtained healthy bacterial culture which was used for seeding on the samples for quantitative and qualitative assessments of antibacterial response. Statistical analyses were done for the comparison of outcomes among all the non-polarized and polarized samples. For this purpose, SPSS 20 software with one-way analyses of variance (ANOVA) and tukey test ($p < 0.05$) was used.

3.11.1. Quantitative analyses

3.11.1.1. MTT assay

MTT assay was used to measure the viability of *E. coli* and *S. aureus* bacterial cells on the non-polarized and polarized $Na_xK_{1-x}NbO_3$ as well as HA samples. The samples were seeded with 150 µl of 0.1 OD bacterial culture in 350 µl of respective media and incubated for 10 h at 37 °C. After incubation, the culture was removed from the samples which was followed by washing with 1x phosphate buffer saline (PBS) to remove media debris and dead bacterial

cells. Afterward, 500 µl of reconstituted MTT (MTT: 1x PBS as 1: 10) was added to each well (24 well tissue culture plate) and further incubated for 2 h at 37 °C to allow for the formation of formazan crystals. Now, MTT from each sample was replaced by dimethyl sulfoxide (DMSO) to dissolve formazan crystals and the OD of these dissolved formazan crystals was measured using ELISA microplate reader (Bio-red) at 595 nm which represents the viability of bacterial cells [21, 22]. In addition, the antibacterial ratio for *E. coli* and *S. aureus* bacteria on non-polarized and polarized $Na_xK_{1-x}NbO_3$ and HA samples were calculated as (Eqn. 3.11) [23],

$$\text{Antibacterial ratio (\%)} = \frac{OD_{Blank} - OD_{Sample}}{OD_{Blank}} \times 100 \qquad (3.11)$$

3.11.2. Qualitative analyses

3.11.2.1. Fluorescence imaging

The presence of live and dead bacteria has been observed using a fluorescence microscope (Nikon Eclipse, LV 100 ND). SYTO 9 (excitation/emission is 480/500 nm) and propidium iodide (PI, excitation/emission is 490/610 nm) were used to stain live and dead bacterial cells, respectively. For this experiment, non-polarized and polarized samples of $Na_xK_{1-x}NbO_3$, as well as HA, were seeded with *E. coli* and *S. aureus* bacterial cells with 0.1 OD for 10 h at 37 °C. After incubation, the bacteria seeded samples were washed with 1x PBS and a small drop (1 - 2 µl) of the mixture of both the dyes (SYTO 9: PI in the ratio of 1: 1) was added to stain the cultured samples.

3.11.2.2. Disk diffusion method

The antibacterial potential of non-polarized and polarized $Na_xK_{1-x}NbO_3$, as well as HA samples, were examined using the disk diffusion method. For this experiment, the samples were seeded with *E. coli* and *S. aureus* bacterial cells with 0.1 OD in 24 well plates for 10 h

at 37 °C. After incubation, samples were removed from the wells and the culture was diluted 1000 times in 1x PBS. Following this, 100 µl of diluted culture was smeared in the agar plate (Surface area: 58 cm^2) using L rod and again incubated for 12 h at 37 °C. After specific incubation, bacterial colonies, formed on the agar plate, were counted by the digital colony counter and images were captured using a digital camera. The antibacterial ratio for both the bacteria on non-polarized and polarized $Na_xK_{1-x}NbO_3$ as well as HA samples was calculated as (Eqn. 3.12) [24],

$$\text{Antibacterial ratio (\%)} = \frac{N_B - N_S}{N_B} \times 100 \qquad (3.12)$$

Where, N_B and N_S are the number of colonies, formed on blank and sample, respectively.

3.12. *In vivo* assessment of systematic toxicity of nano-sized NKN powder

In view of the implant debris associated inflammation, dissemination in distal organs, aseptic loosening etc., the compatibility of debris particles of implant, with blood/tissue is essential to study even if the implant exhibits good biocompatibility in bulk form.

In view of the above, the present study made the first attempt to elucidate *in vivo* toxicity of various compositions of (Na, K) NbO_3 nanoparticles in rats' model as a step ahead toward the development of piezoelectric NKN-based prosthetic orthopedic implant.

3.12.1. Nano-sized powder preparation

The $Na_xK_{1-x}NbO_3$ (x = 0.2 - 0.8) powders of micron-level particle size were prepared using the solid-state method. The detailed synthesis procedure for NKN has been demonstrated in section 3.1.1. The particle size for the calcined powder of $Na_xK_{1-x}NbO_3$ were ranges from ~ 400 – 700 nm. The particle size was further reduced to nano-size using a high-energy planetary ball mill (Fritsch Pulverisette 5) in an ethanol medium for 10 h at 300 rpm. Zirconia balls were used as a grinding tool and the balls to powder ratio was kept at 10:1.

3.12.2. Characterization of nano-powders

The phase evolution analyses of ball-milled nano-sized $Na_xK_{1-x}NbO_3$ powder were done using the X-ray diffraction (XRD, Rigaku Miniflex II Desktop X-ray Diffractometer) technique with Cu-Kα (wavelength, λ = 1.5406 Å) radiation. The morphology and particle size of the ball-milled powders were further examined using high-resolution scanning electron microscopy (Nova Nano SEM, FEI). The energy dispersive X-ray spectroscopy (EDS) was performed to evaluate the elemental distribution in NKN powders. The particle size distribution of the prepared NKN powders in aqueous media was examined via the dynamic light scattering method using a particle size analyzer (Zetasizer nano range, Malvern).

3.12.3. Preparation of eluate solution

Primarily, the ball-milled nanopowder of $Na_xK_{1-x}NbO_3$ was sterilized using a steam autoclave at 120 °C for 30 min. Thereafter, three different concentrations of 0.25, 2.5 and 25 mg/ml were prepared by the suspension of each composition of NKN in saline (0.9 % w/v NaCl). Saline was used as a vehicle for the injection of nanoparticles in rats. Different compositions of NKN nanoparticulates i.e., $Na_xK_{1-x}NbO_3$ (x = 0.2, 0.5, 0.8) were designated as N1, N2 and N3, respectively. However, the concentrations 0.25, 2.5 and 25 mg/ml were marked as C1, C2 and C3. Before injection, the eluates were ultrasonicated for 10 min at the interval of 6 h up to 2 days for homogeneous dispersion. The homogenized eluates were further autoclaved to ensure sterilized injection.

3.12.4. Cell - NKN nanoparticles interaction

In vitro cell culture experiments were performed to evaluate the viability of MG-63 cells on the eluates of $Na_xK_{1-x}NbO_3$ nanoparticulates. The cells were prepared for culture as

demonstrated in section 3.10. The cells were seeded at a density of 10^4 cells/ml on the gelatin-coated glass coverslip and incubated for 12 h. After a stipulated period of time, the wells having adhered cells were exposed with 100 µl of three different concentrations C1, C2 and C3 of N1, N2 and N3 samples in each well. In addition, the same amount of saline was added to the wells with adhered cells which was used as control (marked as Cs). Again, the samples were incubated in the respective media at 37 °C (5% CO_2, 95 % relative humidity) to examine the quantitative (MTT assay) and qualitative (fluorescence imaging) cellular response, after 24 and 72 h of seeding.

MTT [3-(4, 5-dimethylthiazol-2-yl)-2, 5-diphenyl-tetrazolium- bromide)] assay was performed after 24 and 72 h on the C1, C2, C3 concentrations of N1, N2 and N3 samples and saline. After incubation, the culture was removed from each well and washed twice with 1x PBS solution. Thereafter, the reconstituted MTT (MTT: media in the ratio of 1:10) was added to each well having samples and control and again incubated the samples at 37 °C (5% CO_2, 95 % relative humidity) for 6 h to form formazan crystals by the reaction of MTT with live cells. After this, the MTT solution of each well was replaced by DMSO and again incubated for 10 minutes to dissolve the formazan crystals. The amount of these formazan crystals was measured in terms of optical density at 595 nm by using ELISA Microplate (iMark Bio-rad) reader.

The adherence and morphology of MG-63 cells on the eluates of $Na_xK_{1-x}NbO_3$ and saline control samples were observed using fluorescence microscopy for 24 and 72 h. The procedure for staining the nucleus and cytoskeleton of cells, adhered to the nano-particles treated wells was similar as demonstrated in section 3.10.2. Thereafter, the cells were observed using a fluorescence microscope (Nikon Eclipse LV 100 ND).

3.12.5. Animal study

In the present study, male Wistar rats (average weights; 200±20 g) were procured from the Central Animal House, Institute of Medical Science, Banaras Hindu University (BHU), Varanasi. The animal study was approved by the Institutional Animal Ethical Committee of BHU (Approval No.: BHU/DoZ/IAEC/2021-2022/034). The animals were housed in standard conditions as suggested by the animal ethical committee such as controlled humidity (45-55 % RH) and temperature (25 ± 1 °C), proper ventilation and half-day light/dark cycle. The animals were kept for one week before the experiment to habituate them with the environment. The animals were divided into five groups as control, saline and particulate eluates treated groups (N1, N2 and N3) in which each group contains 6 rats. The animals were injected with 100 µl of particulates eluate (25 mg/ml) and pure saline. The furs on the knee of the rats were removed carefully. Before injection, the rats were anesthetized using Thiopentone (dose: 40 mg/kg body weight; i.p.), followed by intra-articular injection of prepared eluates [Fig. 3.5].

Fig. 3.5. Demonstration of intra-articular injection of NKN nanoparticulates in the knee (synovial) joint of Wistar rat.

3.12.5.1. General observation

Changes in skin, furs, salivation, diarrhea, tremor, convulsion and comatose conditions were monitored throughout the experimental protocol. The weight of rats was also monitored on day 1, 3, and 7 of injection. At the end of the 7^{th} day, the rats were sacrificed by decapitation and blood was collected for biochemical analyses. The retrieved blood samples were centrifuged at 3000 rpm (REMI, NEYA 16R, India) at 4 °C, to extract the serum. The obtained serum was preserved at – 80 °C for further biochemical assays [Fig. 3.6]. Various organs like, heart, liver, kidney, spleen and knee were collected from the rats of each group and washed with 1x PBS twice. The retrieved organs were instantly fixed in 10 % formalin buffer for histopathological and inflammatory tests [Fig. 3.6].

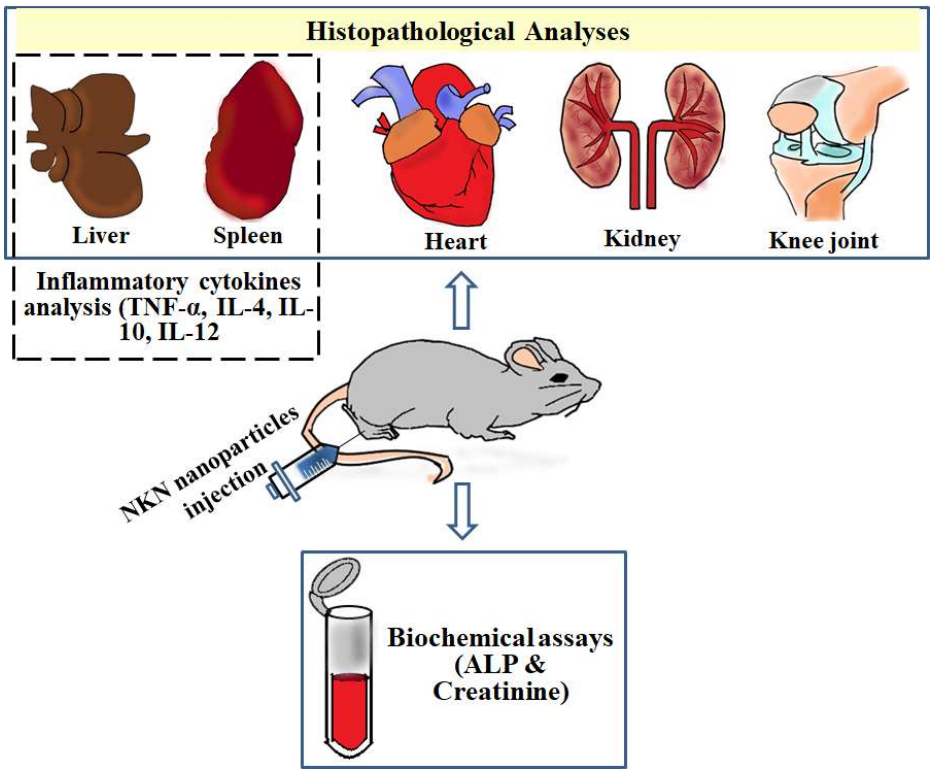

Fig. 3.6. Schematic illustration of in vivo studies performed after intra-articular injection of $Na_xK_{1-x}NbO_3$ nanoparticles for 7 days. The histological analysis was done for the heart, liver, kidney, spleen and knee joint to for the inspection of microscopic changes in such organs. The inflammatory cytokines were examined on liver and spleen tissues to observe the level of inflammation after particulate injection. The blood serum extracted from the rats was used for biochemical assays (ALP and Creatinine) to analyze the cellular metabolism.

3.12.5.2. Biochemical assay for serum assessment

The serum, collected from the $Na_xK_{1-x}NbO_3$ particulates injected and control groups of rats, were biochemically analyzed for the assessment of alkaline phosphatase (ALP) and Creatinine activities. For ALP activity, a commercially available diagnostic kit, named, AUTOSPAN Liquid and MBK Alkaline phosphatase kit (ARKRAY healthcare Pvt. Ltd, India) was used and the experiments were performed following the manufacturer's protocol.

The creatinine rat assay kit (Crystal Chem, IL, USA) was used to examine the creatinine level and the experiment was performed according to the manufacturer's protocol.

3.12.5.3. Inflammatory test with organs

3.12.5.3.1. Inflammatory cytokines profiling

The spleen and liver of the $Na_xK_{1-x}NbO_3$ particulate treated (N1, N2 and N3) and control groups of rats were collected for cytokine profiling. Primarily, RNA isolation was done from the tissues of animals [25]. The spleen and liver are secondary lymphoid organs, housing T_0 cells and antigen-presenting cells (Mϕ & DCs) and these cells optimally respond against foreign invaders [26]. Therefore, inflammatory analyses were performed with these organs. For this purpose, trizol (Invitrogen) of 1 ml/50-100 mg tissue was added to each tissue which solubilizes and denatures their proteins. Thereafter, chloroform (200 µl/ml trizol) was added to the solution and the solution was centrifuged at 10000 rpm for 15 min (at 4 °C) which resulted in the separation of protein, DNA and RNA in three layers. The RNAs, present in the aqueous phase, were precipitated using isopropanol (500 µl/ml solution) and further, the solution was centrifuged at 10000 rpm for 10 min (at 4 °C). The obtained RNA pellet for each sample was washed using 70 % ethanol, followed by drying. Further, the dried RNA was dissolved in nuclease-free water and then the purified RNA was stored in ethanol at – 20 °C which was later on used for quantification in Nano-drop 1000. For the synthesis of cDNA, 2 microgram of RNA for each sample were allowed to pass through reverse transcription with 20U M-MLV reverse transcriptase (Fermantas, Germany), 20 mM dTNP (New England Biolabs, USA), 1 X RT buffer, 0.1 M DTT in DEPC treated or nuclease-free water, and 100 ng of random hexamers (Fermentas, Germany) [27, 28]. For real-time PCR analyses, the reaction mixture was prepared using 2 µl of nuclease-free water, 5 µl of syber green (Applied

Biosystem), 1 µl of cDNA, 1 µl RNase inhibitor, 0.5 µl of reverse and forward primer each [27, 29]. The PCR conditions were maintained based on the previous literature report [27]. Thereafter, the expression levels of pro-inflammatory cytokines (TNF-α and IL-12) and anti-inflammatory cytokines (interleukin or IL-4 and IL-10) were estimated for NKN treated, saline treated and non-injected organ samples. The data sets were normalized to GAPDH (Invitrogen) which is used as an internal control. The gene expressions were calculated in fold change using Δ^2CT method.

3.12.5.3.2. Histopathological analyses

The fixed tissues such as the heart, spleen, liver and kidney were dehydrated using ethanol solution. Thereafter, paraffin blocks were fabricated by embedding tissues in paraffin wax. The embedded blocks of tissues were sectioned (10 µm) and then stained using hematoxylin and eosin (H&E) stains for histopathological analyses. The fixed knee joint tissues were decalcified using 10 % nitric acid solution and then dehydrated using ethanol solution. The embedded blocks of knee joint tissues were prepared for H & E analyses similar to other organs. The images of stained tissues were observed using a fluorescence microscope (Nikon Eclipse LV 100 ND).

3.12.6. Statistical analyses

The statistical analysis among the samples was done using SPSS (statistical package for social sciences, IBM) software. In addition, the significant difference among the samples was identified using ANOVA technique. Tukey and Games–Howell tests at $p \leq 0.05$ were used for the post hoc multiple comparisons.

Optimally processed disc shaped samples of $Na_xK_{1-x}NbO_3$ (x = 0.2-0.8) and HA are used for various targeted studies. XPS and contact angle measurement are carried out to examine the

effect of polarization on surface chemistry and wettability. *In vitro* studies are performed to analyze the biocompatibility and antibacterial response of electrically modified $Na_xK_{1-x}NbO_3$. For this purpose, the synergistic effect of variation of Na and K contents, surface polarization and external electrical stimulation on the cellular response are investigated. In this study, osteogenic response of osteoblast-like cells such as MTT assay, florescence imaging, alkaline phosphatase activity and intracellular calcium ions measurement are performed. In addition, the influence of surface polarization along with the variation in Na and K contents on the antibacterial response are analyzed. *In vivo* toxicity assessments are also performed on the NKN nanoparticles such as histopathological analyses, inflammatory cytokines profiling and biochemical assays (ALP and creatinine).

References

[1] B. Malic, A. Benan, T. Rojac, M. Kosec, Lead-free Piezoelectrics Based on Alkaline Niobates: Synthesis, Sintering and Microstructure, Acta Chim. Slov. 55 (2008) 719-726.

[2] M. H. Santos, M. Oliveira, L. P. F. Souza, H.S. Mansur, W. L. Vasconcelos, Synthesis control and characterization of hydroxyapatite prepared by wet precipitation process, Mater. Res. 7 (2004) 625-630.

[3] Q. Wang, J. Yang, W. Zhang, R. Khoie, Y. M. Li, J. G. Zhu, Z. Q. Chen, Manufacture and Cytotoxicity of a Lead-free Piezoelectric Ceramic as a Bone Substitute-Consolidation of Porous Lithium Sodium Potassium Niobate by Cold Isostatic Pressing, Int. J. Oral Sci. 1(2009) 99-104.

[4] S. Sarkar, R. Das, Shape effect on the elastic properties of Ag nanocrystals, Micro Nano Let. 13 (2018) 312–315.

[5] M. A. Tagliente, M. Massaro, Strain-driven (002) preferred orientation of ZnO nanoparticles in implanted silica, Nucl. Instrum. Methods Phys. Res. B. 266 (2008) 1055–1061.

[6] R. Jacob, J. Isac, X-ray diffraction line profile analyses of Ba0.6Sr0.4FexTi1-x O3-δ, Int. J. Chem. Studies 2 *(*2015) 12-21.

[7] K. A. Zak, A. W. H. Majid, M. E. Abrishami, R. Yousefi, X-ray analysis of ZnO nanoparticles by Williamson-Hall and size-strain plot methods, Solid State Sci. 13 (2011) 251.

[8] ASTM E3484-99 A. Standard test method for micro indentation hardness of materials, (1984).

[9] A. Oyane, H. M. Kim, T. Furuya, T. Kokubo, T. Miyazaki, T. Nakamura, Preparation and assessment of revised simulated body fluids, J. Biomed. Mater. Res. 65A (2003) 188–195.

[10] N. Yamada, T. Okano, H. Sakai, F. Karikusa, Y. Sawasaki, Y. Sakurai, Thermoresponsive polymeric surfaces – control of attachment and detachment of cultured-cells. Makromol Chem-Rapid 11 (1990) 571–576.

[11] P. G. Robey, The Biochemistry of Bone, Endocrinology and Metabolism Clinics of North America, 18 (4) (1989) 859-902.

[12] E. E. Golub, K. B. Battaglia, The role of alkaline phosphatase in mineralization. Curr. Opin. Orthop. 18 (2007) 444–448.

[13] N. S. Fedarko, P. Bianco, U. Vetter, P. Gehron Robey, Human Bone Cell Enzyme Expression

and Cellular Heterogeneity : Correlation of Alkaline Phosphatase Enzyme Activity With Cell Cycle, J. Cell. Physiol. 114 (1990) 115–121.

[14] D. Khare, B. Basu, A. K. Dubey, Electrical stimulation and piezoelectric biomaterials for bone tissue engineering applications, Biomaterials 258 (2020) 120280.

[15] N. More, G. Kapusetti, Piezoelectric material - a promising approach for bone and cartilage regeneration, Med. Hypotheses 108 (2017) 10–16.

[16] M. D. Bootman, M. J. Berridge, H. L. Roderick, Calcium signalling: more messengers, more channels, more complexity, Curr. Biol. 12 (2002) 563e5.

[17] G. Song, G. Ouyang, S. Bao, The activation of Akt/PKB signaling pathway and cell survival, J. Cell Mol. Med. 9 (2005) 59e71.

[18] S. Staehlke, A. Koertge, B. Nebe, Intracellular calcium dynamics dependent on defined microtopographical features of titanium, Biomaterials 46 (2015) 48-57.

[19] Y. Shao, M. Alicknavitch, M. C. Farach-Carson, Expression of voltage sensitive calcium channel (VSCC) L-type Cav1.2 (alpha1C) and T-type Cav3.2 (alpha1H) subunits during mouse bone development, Dev. Dyn. 234 (2005) 54e62.

[20] D. F. Virgilio, T. H. Steinberg, S. C. Silverstein, Inhibition of Fura-2 sequestration and secretion with organic anion transport blockers, Cell Calcium 11 (1990) 57–62.

[21] A. A. V. de Loosdrecht, R. H. J. Beelen, G. Ossenkoppele, M. G. Broekhoven, M. M. A. C. Langenhuijsen, Tetrazolium-Based Colorimetric MTT Assay to Quantitate Human Monocyte Mediated Cytotoxicity Against Leukemic Cells from Cell lines and Patients with Acute Myeloid Leukemia, J. Immunol. Meth. 174 (1994) 311-320.

[22] Y. B. Liu, D. A. Peterson, H. Kimura, D. Schubert, Mechanism of cellular 3-(4,5 dimethylthiazol-2-yl)-2,5- diphenyltetrazolium bromide (MTT) reduction, J Neurochem. 69 (1997) 581-593.

[23] C. Xie, X. Lu, L. Han, J. Xu, Z. Wang, L. Jiang, K. Wang, H. Zhang, F. Ren, Y. Tang, Biomimetic Mineralized Hierarchical Graphene Oxide/Chitosan Scaffolds with Adsorbability for Immobilization of Nanoparticles for Biomedical Applications, ACS Appl. Mat. Interf. 8 (2016) 1707-1717.

[24] T. Yao, J. Chen, Z. Wang, J. Zhai, Y. Li, J. Xing, S. Hu, G. Tan, S. Qi, Y. Chang, P. Yu, C. Ning, The antibacterial effect of potassium-sodium niobate ceramics based on controlling piezoelectric properties, Coll. Surf. B: Biointerfaces 175 (2019) 463–468.

[25] D. C. Rio, M. Jr Ares, G. J. Hannon, T. W. Nilsen, Purification of RNA using TRIzol (TRI reagent). Cold Spring Harb Protoc. 6 (2010) pdb.prot5439.

[26] R. Singh, A. Anand, A. K. Rawat, S. Saini, B. Mahapatra, N. K. Singh, A. K. Mishra, S. Singh, N. Singh, D. Kishore, V. Kumar, P. Das, R. K. Singh, CD300a Receptor Blocking

Enhances Early Clearance of *Leishmania donovani* From Its Mammalian Host Through Modulation of Effector Functions of Phagocytic and Antigen Experienced T Cells, Front. Immunol. 12 ((2022) 793611.

[27] A. K. Rawat, K. Pal, R. Singh, A. Anand, S. Gupta, D. Kishore, S. Singh, R. K. Singh, The CD200-CD200R cross-talk helps Leishmania donovani to down regulate macrophage and CD4+CD44+ T cells effector functions in an NFκB independent manner, Int. J. Biolog. Macromol. 151 (2020) 394-401.

[28] H. Birla, S. N. Rai, S. S. Singh, W. Jahra, A. Rawat, N. Tiwari, R. K. Singh, A. Pathak, S. P. Singh, Tinospora cordifolia Suppresses Neuroinflammation in Parkinsonian Mouse Model. Neuromol Med 21 (2019) 42–53.

[29] A. Peinnequin, C. Mouret, O. Birot, A. Alonso, J. Mathieu, D. Clarençon, D. Agay, Y. Chancerelle, E. Multon, Rat pro-inflammatory cytokine and cytokine related mRNA quantification by real-time polymerase chain reaction using SYBR green, BMC immunology 5 (2004) 3.